APPLICATION OF THE COUPLED THREE DIMENSIONAL THERMAL-HYDRAULICS AND NEUTRON KINETICS MODELS TO PWR STEAM LINE BREAK ANALYSIS

Michel GONNET and Michel CANAC
FRAMATOME
Tour Framatome. Cedex 16, Paris-La Défense, 92084, France.
mgonnet@framatome.fr ; mcanac@framatome.fr

ABSTRACT

The 3D thermal-hydraulic (T/H) code, FLICA 3-F[1], has been coupled with Framatome's modular nodal code, SMART[2], which is part of SCIENCE[3], a comprehensive integrated system for core physics calculation. FLICA 3-F is Framatome's standard code for core T/H calculations. This paper describes briefly both the neutron and T/H models and emphasizes physical results obtained in the main steam line break (MSLB) simulation and the benefits of using a coupled approach.

1. INTRODUCTION

The core T/H code FLICA is used for the DNBR (departure from nucleate boiling ratio) calculation. In the uncoupled approach, the 3D-power shape is obtained from a neutron kinetics computation including a water density feedback predicted by a simple closed channel model. In such an approach, the 3D T/H effects have no influence on neutron flux shape behavior. The closed channels computation generally overestimates water density gradients so it leads to over-estimation of the power peaking factor. This feature leads generally to some conservatism in accident analysis and particularly in the MSLB transient study. Therefore Framatome has introduced a 3D T/H model in its core physics computational system, SCIENCE. The FLICA 3-F code has been modularized and is a part of 3D kinetics nodal code, SMART. The aim of FLICA, in this environment, is on the one hand, to handle nodal water density computation in steady state or transient calculations, and on the other hand, to perform DNBR calculation in a set of given assemblies.

2. MODELS OVERVIEW

2.1 NEUTRON MODEL

The SMART neutron model solves both the static and time-dependent neutron diffusion equations in two-energy groups. Spatial integration uses the nodal expansion method, with polynomial combined with hyperbolic terms to represent the transverse integrated fluxes. Transverse leakage fluxes are represented by a quadratic polynomial. Nodal cross sections are represented by quadratic terms in each spatial direction in both the neutron balance and the transverse leakage equations. Assembly discontinuity factors are utilized to correct the homogenization errors. The theta method is used for time integration, allowing fully explicit, semi-implicit or fully implicit treatments. The precursor equations account for six groups of delayed neutrons. Dynamic frequencies are utilized to eliminate the time dependence of the flux expansion coefficients in the transverse integrated flux equations. Both assembly and quadrant pin reconstruction methods are available, based on single assembly lattice calculations.

2.2 FUEL THERMAL MODEL

The SMART fuel pin model solves the one-dimensional, time-dependent, radial heat conduction equation. The fuel pellet radial temperature distribution is calculated by iterating on material properties, pellet-to-clad conductance, and radial ring temperatures. The gap conductance is determined as a function of the fuel rod properties. The heat conduction equation is solved using centered mesh, finite difference equations and the Crank - Nicholson method.

2.3 FLICA 3-F T/H MODEL

FLICA 3-F is a 4-equation two-phase flow with slip ratio model. It enables steady state and transient calculations in a reactor core. The momentum balance equation accounts for cross flow between channels. The main assumptions allowing simplifications in Navier – Stokes equations are the following: the thermal conductivity and the turbulent diffusion are taken into account in radial directions and neglected in axial direction; the liquid phase is supposed to be incompressible; the two phases are characterized by the mass, momentum and enthalpy of the mixture and by the enthalpy of the liquid phase; an algebraic slip ratio model describes differential velocities between liquid and steam phases.

3. MAIN STEAM LINE BREAK TRANSIENT

Initiating event for class 4 accident is the postulated double ended guillotine break of one main steam line connecting the steam generator (SG) to the turbine. Following such rupture, large steam release coming from both faulted SG and intact SG, as long as main steam isolation valves are still open, provides large overcooling of the reactor coolant and drop of pressurizer level and pressure. The reactor protection system actuates automatic reactor trip upon receipt of advanced low SG pressure signal. During reactor power operation, fast control rod insertion allows for rapid core power decrease despite the reactivity insertion caused by the core cooling down.

Starting from hot nominal power conditions, part of total MSLB energy removal is used for reactor cooling down to zero power conditions. Hot zero power conditions do not provide such energy to be removed by the MSLB: therefore, such initial conditions result in stronger reactor cool down, and appear more limiting in terms of reactivity insertion and potential core power retrieval. Rapid reactor pressure drop combined with significant core power might lead to departure from nucleate boiling.

The core power level and power distribution are strongly dependent on the water density and Doppler feedback. Imperfect loop flow mixing results in heterogeneous temperature distribution at core inlet. Such heterogeneity is amplified by the usual safety assumption of one stuck control rod. These conditions result in a strong heterogeneous core power distribution and therefore in a strong coupling in thermal-hydraulics and neutronics.

4. BENEFITS OF THE COUPLED APPROACH

4.1 METHODOLOGY

The behavior of nuclear and thermal power during the MSLB transient is shown on Figure 1.

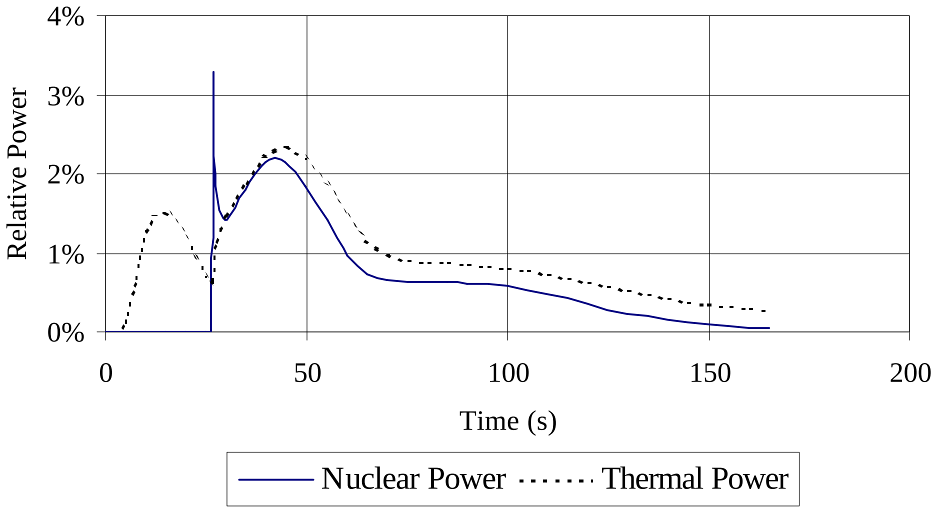

Figure 1: Core Power Level vs. Time during MLSB Transient

The transient is initiated at hot zero power conditions with all rods in except one stuck rod. The initial reactivity is adjusted at the minimum value of reactivity shutdown margin. In the given example, the primary coolant pumps have been supposed to shutdown at t=0 (see Figure 2). The cooling of the fuel produces the first thermal power maximum at nearly 15s. The reactor becomes prompt critical at about 20s producing a sharp peak of nuclear power limited by the Doppler effect. The amount of energy released during the prompt critical phase produces a new increase in thermal power, which slightly exceeds the nuclear power level. The cooling down of the reactor continues, and the nuclear power is still increasing. In the case shown on Figure 1, the assumption of a very efficient safety injection was made (see Figure 3). Therefore, the increase in nuclear power is stopped by the massive arrival of boron into the core near 70 seconds.

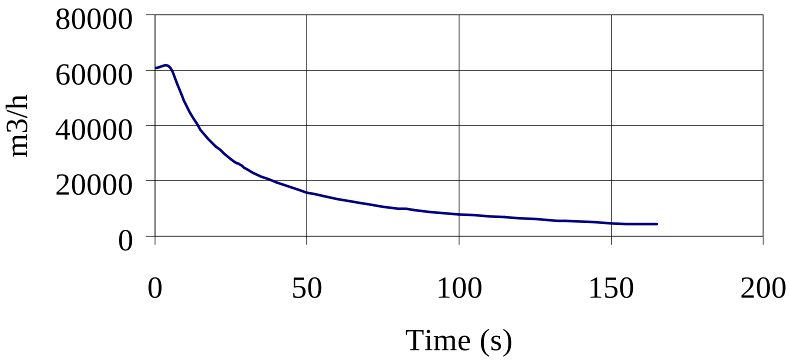

Figure 2: Volumic Flow Rate vs. Time

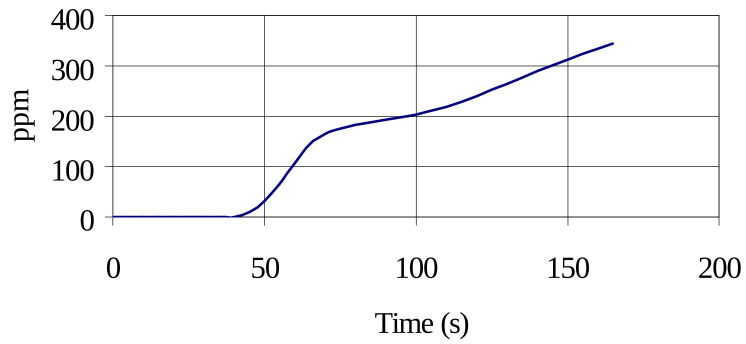

Figure 3: Boron Concentration vs. Time

Despite pessimistic initial conditions, the assumptions made for the transient lead to a very low core power level and the DNB risk is out of the question. Nevertheless, depending on the reactor design, the reachable maximum power level may be significantly higher. To cover the set of possible transient simulations, numerous design parameters would have to be considered. For instance, we would have to consider the power level extracted from the steam generator (SG), the initial mass of water in the SG, the safety injection system design (pumps pressure and boron concentration), the shutdown or otherwise of the primary pumps, the core reload design, the choice of the stuck rod etc… The combination of these parameters would lead to a prohibitive number of transients to be analyzed. As we are focusing on the potential benefits of the 3D T/H coupling in the most generic case (without any assumption on the plant design), the range of possible situations was approached by a sensitivity study on core power level and mass flow rate. Imposing given core conditions requires steady state calculations and the question of the significance of such an approach is raised. The analysis of typical MSLB transients shows that the core is not far from steady state at the time of maximum thermal power. Therefore, the conclusions made from the state point analysis can be extended to the transient case.

4.2 HIGH FLOW RATE CASES

Because of postulated stuck rod and imperfect loop flow mixing, the core behavior is governed by the existing conditions limited to some assemblies surrounding the stuck rod location. Most of the nuclear power is generated inside this zone and, depending on the core power level, inside only a part of that zone. At zero power, the power axial offset (AO) of the core as well as the hot zone is close to 50 or 70%. The AO decreases as soon as the power increases because of the heating of the upper part of the hot zone. The AO remains positive as long as no significant boiling appears in upper part of the hot zone. See the curves at 5 and 10% of nominal power on Figure 4.

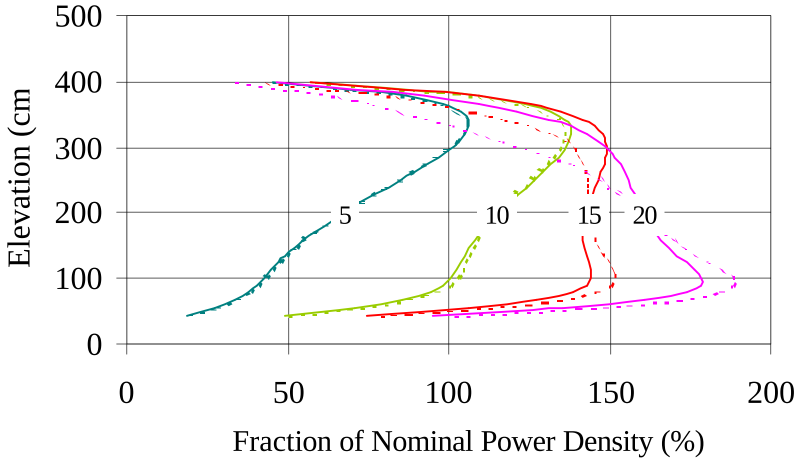

Figure 4: Hot Assembly Power Distribution vs. Core Power Level.
Dashed lines: Closed channel T/H. Solid lines: 3D T/H model.

These curves show that the results provided by both T/H models are approximately the same. The maximum void ratio obtained in the 10% case is less than 1%.

A first conclusion can be made: at nominal flow rate, as long as void ratio in the upper part of the hot assembly is low, the coupled and uncoupled approaches are equivalent.

When the core power level increases (see 15 and 20% curves on Figure 4), the increasing water density offset in the hot assemblies pushes the power down the core. In such conditions, the responses of 3D and 1D T/H models begin to differ. The power redistribution in the low part of the core is amplified when computed with the closed channel model. For example at 20% of nominal power, we notice that the closed channel calculation overestimates the maximum assembly power by about 6%.

The differences between the two calculations can be explained by observing the cross flow distribution along the hottest channel. The curve labeled “G” on Figure 5 is the relative difference between local mass velocity and inlet mass velocity. A positive value of G indicates that the fluid is entering the channel. The density drop resulting from the boiling in the upper part of the channel is responsible for an increase in axial pressure loss due to frictions. The resulting increase in local pressure produces a strong ejection of the fluid into adjacent channels. Consequently, the redistribution of flows in the surrounding zones leads to an entering flow at the lower part of the boiling section. The ejection of hot water and steam in the upper part of the channel in addition to the entering of "cold" water at the beginning of boiling section contributes to a significant decrease in the local fluid enthalpy.

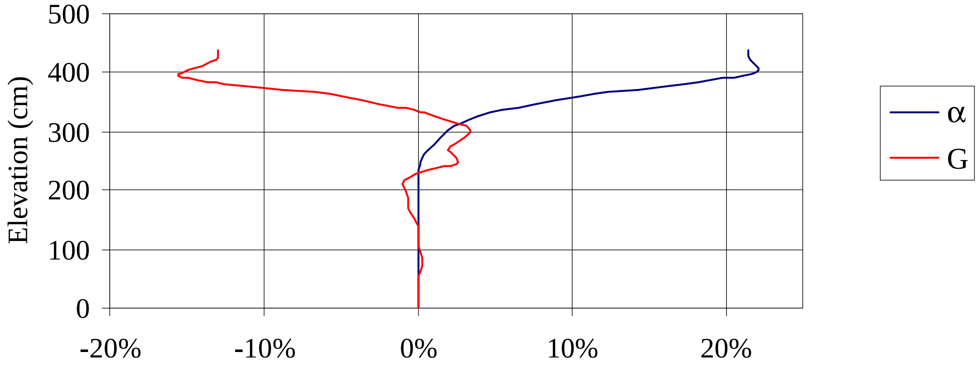

Figure 5: Void Fraction (α) and Relative Mass velocity (G) vs. Elevation

Figure 6 compares the axial distributions of water density in the hot channel obtained with either the 3D T/H model or the 1D T/H model. The absence of cross flow modeling of closed channel approximation overestimates the void ratio in the upper part of the hot assembly.

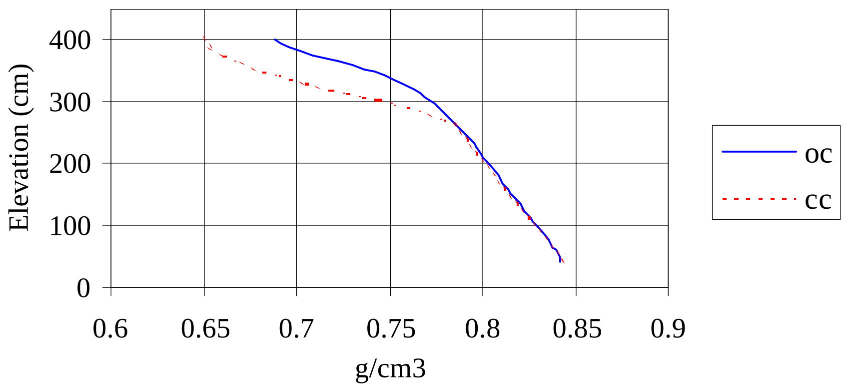

Figure 5: Axial Distribution of Water Density in the Hot assembly
Power: 20%, Flow Rate: 100% obtained whith open channel (oc)
and closed channel (cc) T/H.

The visible effects on axial power distribution have now to be discussed in term of DNB risk. The low power range (up to 10%) can be excluded from the discussion a priori because the two calculations give nearly the same power distribution and the DNBR results will be identical. Moreover, there is no DNB risk in this power range with the given pressure and inlet temperature of the present study. Figure 7 shows the DNBR margin gain provided by the use of the coupled model given as a function of the power level. The DNBR calculation covers the range from 10% to 30% of nominal power. In the low power range, the 1D T/H calculation overestimates the DNBR. The difference between the two results reaches a maximum value of 14% at 15% nominal power. In that particular case, the maximum power density given by the 3D T/H calculation is slightly lower, but it occurs in the upper part of the channel, where the water is not very far from bulk boiling. This feature persists as long as the AO given by the 3D T/H calculation is positive while the one obtained by the 1D T/H is negative. The lack of conservatism of the 1D T/H modeling has no consequence as it occurs in the range where the safety margin is highest (at least 40%).

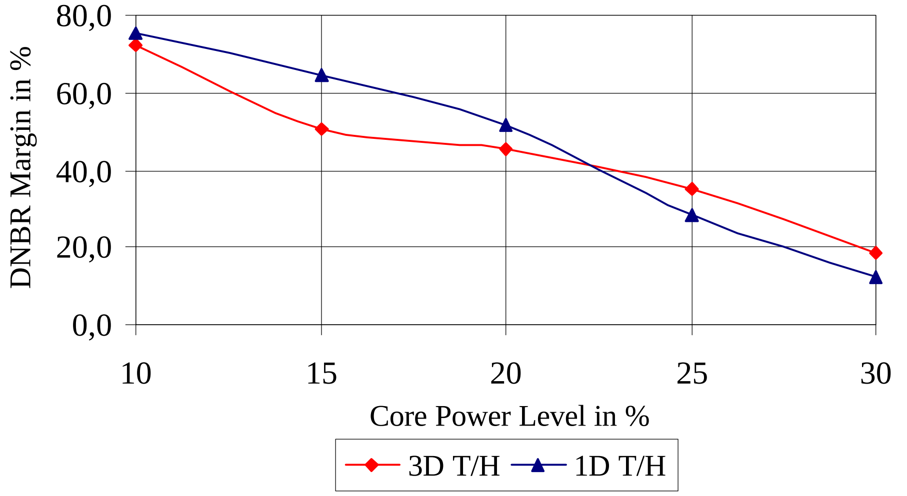

Figure 7: DNBR Margin vs Core Power Level at 100% of Nominal Flow

In the higher power range, where the DNBR margin is the lowest, the 1D T/H calculation leads to a pessimistic result.

To complete this conclusion, we have to take care with the kinetic aspects. Actually, the sensitivity study discussed above was performed with steady state calculations and we have to take into account possible unfavorable reactivity effects.

As it results from the comparison of coupled and uncoupled calculations, the water density in the hot zone is systematically higher when computed with the 3D T/H model. As this zone is the most important from the neutron point of view, one can expect a noticeable increase in reactivity and therefore in core power level reached during the transient. Figure 8 confirms this hypothesis. The reactivity change due to 3D T/H effects reaches about 0.1% at 30% of nominal power. By using the steady state reactivity coefficient, the power increase was found to be lower than 2%. With respect to the DNBR sensitivity to the power level, it is now possible to confirm the less penalizing tendency of coupled 3D T/H calculation.

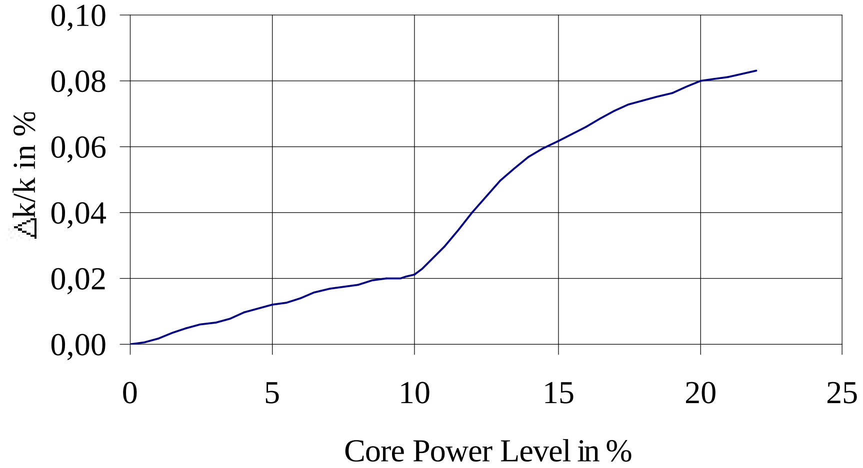

Figure 8: Reactivity change due to 3D T/H effects
At 100% of Nominal Flow Rate.

4.3 LOW FLOW RATE CASES

The eventuality of the shutdown of primary pump may be considered in the MSLB studies. The penalty induced by the use of closed channel analysis in the case of low flow rate was a strong motivation to advance in core coupled modeling.

The sensitivity study performed in the case of full flow was extended to 75%, 50% and 25% flow. The two intermediate cases are not presented here because they do not present any special interest except the demonstration of continuity of phenomena. We will directly focus on the most interesting case of 25% flow.

Figure 9 shows the hot assembly power distribution obtained with both the open channel and the closed channel models for 5% to 20% of nominal power. Because of the low flow rate, the void fraction in the upper part of the hot assembly is sufficient to push the power down the assembly in every case. The AO is now systematically negative, even at 5% power. The closed channel model systematically overestimates the power peaking factor.

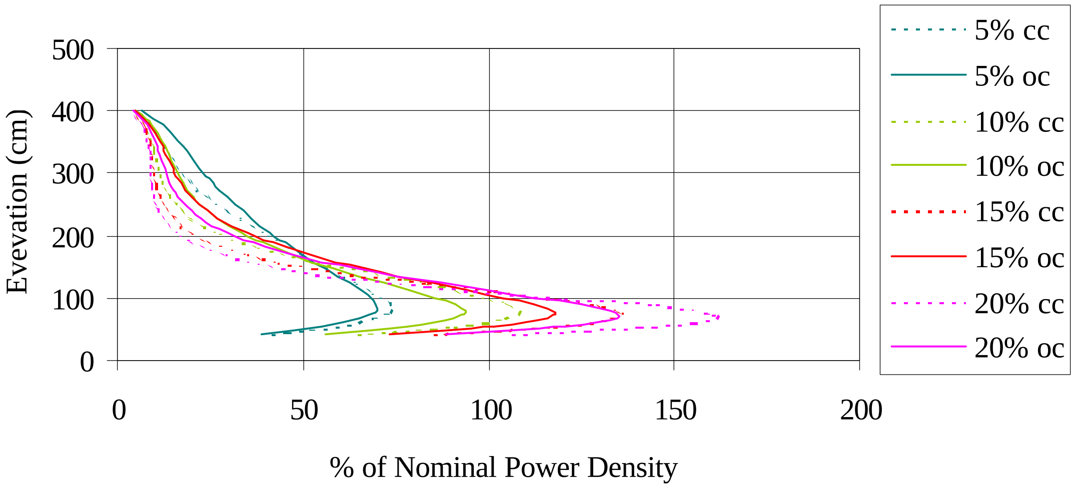

Figure 9: Hot Assembly Power Distribution vs Core Power Level at 25% Flow.

From the neutron point of view, the conclusions made in the full flow case can be extended to the 25% flow case: the cross flows smooth the axial power distribution. Nevertheless, the analysis of detailed T/H results shows that the origin of cross flow is quite different in this case. In the full flow case, the water was ejected from the hot channel because of the increase in friction forces in the boiling section. The flow distribution was mainly conditioned by the frictions. In the 25% flow case, however, the predominant phenomena are the gravity effects. Actually, the gravity forces are responsible for about 75% of total loss of pressure in the channel. So the differences in water weight between the hot channel and its neighbors due to heterogeneity of the water density, induce an increase of axial mass velocity as one can see on Figure 10.

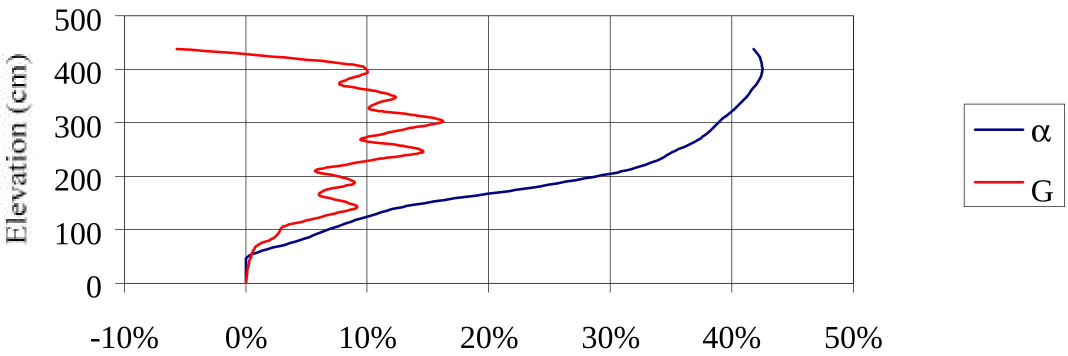

Figure 10: Void Fraction (α) and Relative Mass Velocity (G) vs. Elevation

The oscillations in the cross flow curve correspond to the assembly grids. The void fraction exceeds 40% in the upper part of the channel instead of nearly 20% in the full flow case

Figure 11 shows the axial distributions of water density in the hot assembly obtained with both the coupled and uncoupled models. The difference in outlet water density reaches 0.5 g/cm^3.

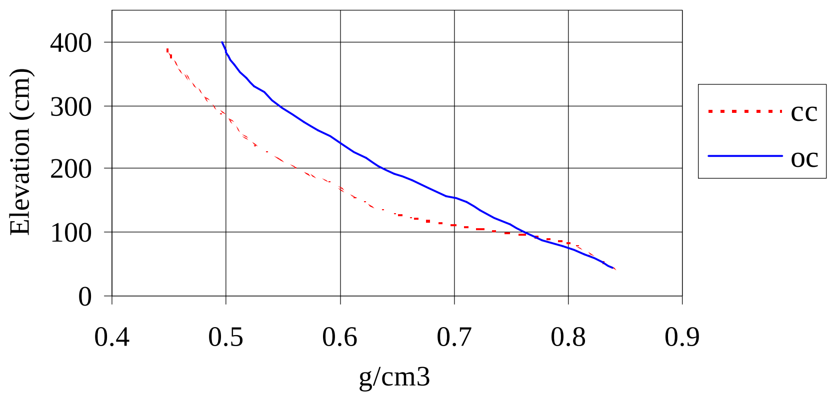

Figure 11: Axial Distribution of Water Density in the Hot assembly
Power: 20%, Flow Rate: 25% obtained whith open channel (oc)
and closed channel (cc) T/H.

Figure 12 shows the DNBR margin gain introduced by the use of the coupled model given as a function of the power level in the 25% flow case. The DNBR calculation covers the range from 5% to 20% of nominal power. In the low flow rate case, the DNBR given by the 3D T/H calculation is systematically greater than the one obtained with the closed channel model.

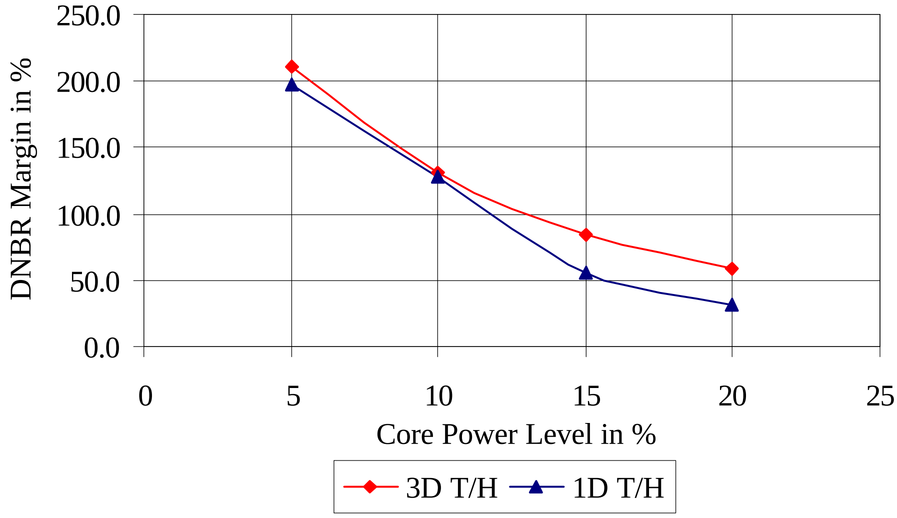

Figure 12: DNBR Margin vs Core Power Level at 25% of Nominal Flow

The difference in margin reaches nearly 30% at 20% of power. The power increase introduced by the reactivity effect in the transient case is less than 3% and the gain in DNBR provided by the use of the coupled calculation exceeds 20%.

CONCLUSIONS

The core 3D T/H code, FLICA 3-F, has been coupled with Framatome's modular nodal code, SMART. The coupling between 3D neutronics and T/H allows more realistic modeling of reactor transients. The application of this approach to safety analysis studies brings to light additional safety margins inherent in simplified modeling. This is particularly true for the MSLB transient because of the strong coupling between neutronics and core T/H involved in such a transient.

The sensitivity study discussed in the present work indicates the contribution of 3D coupled calculations in the analysis of the MSLB transient, and particularly in the case of primary pumps shutdown. The gain in DNBR margin provided by the coupled model ranges from a few percent, in the case of nominal flow rate, to more than 20% at reduced flow.

ACKNOWLEDGEMENTS

The authors wish to acknowledge the SMART developing team and particularly A. Dall’Osso (Framatome) who supervised the code coupling.

REFERENCES

1. JP Bourteele, 1991, internal technical report: FRATEC307E Technical Description of FLICA III-F - Justification for choice of basic models.

2. Hobson, G. H., Gonnet, M. J., Aigle, R. C., 1996. Nodal Kinetics Capability for SCIENCE/NEMO, Physor'96.

3. P. Girieud, “SCIENCE: The New FRAMATOME 3D Nuclear Code Package for Safety Analysis”. Proceeding of the ENC’94 Meeting. Lyon France. October 1994.